Field characterization of vertical bromide transport in a fractured glacial till

William G. Harrar · Lawrence C. Murdoch ·
Bertel Nilsson · Knud Erik S. Klint

Abstract A study of the fracture distribution, hydraulic properties, groundwater levels and the transport of bromide was conducted to characterize vertical transport in the oxidized and reduced zones of a fractured glacial till. Detailed vertical profiles of groundwater levels and solute concentrations were obtained over a 4.5-year period. Vertical migration occurred at several time scales, as a low concentration front was rapidly transported at rates of 100–500 m/year ahead of a slower moving main plume, which advanced at rates of 0.2–0.8 m/year. Concentrations in the leading edge of the plume displayed a high degree of spatial variability over short vertical distances through day 1,000. Late in the test, the influence of matrix diffusion became apparent as concentration patterns developed from being irregular to more uniform distributions. Calculations show that the mass within the low concentration plume front accounts for less than 1% of the total solute mass. Simulation of the breakthrough curves using a simple one-dimensional advection-dispersion model of transport in porous media indicates that vertical transport is dominated by advection. Furthermore, the results indicate that vertical transport of solutes in oxidized and reduced zones of the till can be adequately simulated using an equivalent porous media.

Résumé Une étude de la distribution des fractures, des propriétés hydrauliques, des niveaux de l′eau souterraine et du transport des bromures a été menée afin de caractériser le transport vertical dans les zones oxydées et réduites d'un dépôt glaciaire fracturé. Des profils verticaux détaillés des niveaux de l′eau souterraine et des concentrations des solutés ont été obtenus sur une période de 4.5 années. La migration verticale apparaît sur différentes échelles de temps ; un front de faible concentration a été rapidement transporté à une vitesse de 100 à 500 m/an à l′avant d'un panache plus important moins rapide se déplaçant à une vitesse de 0.2 à 0.8 m/an. Les concentrations des solutés à l′avant du panache ont montré un haut degré de variabilité spatiale sur de courtes distances verticales jusqu'au jour 1000. Plus tard dans le test, l′ influence de la diffusion de la matrice est devenue plus apparente dès lors que les concentrations sont passées d'une distribution irrégulière à une distribution plus uniforme. Les calculs montrent qu'au sein du panache de faible concentration, la masse compte pour moins de 1% de la masse totale de solutés. La simulation des courbes de restitution au moyen d'un simple modèle à une dimension du transport par advection dispersion en milieu poreux indique que le transport vertical est dominé par l′ advection. De plus, les résultats indiquent que le transport vertical des solutés dans les zones oxydées et réduites du dépôt glaciaire peut être adéquatement simulé en utilisant un milieu poreux équivalent.

Resumen Se realizó un estudio de la distribución de fracturas, propiedades hidráulicas, niveles de agua subterránea y transporte de bromuro para caracterizar el transporte vertical en las zonas reductoras y oxidadas de un conglomerado glacial fracturado. Se obtuvieron perfiles verticales detallados de niveles de agua subterránea y concentraciones de solutos en un periodo de 4.5 años. Ocurrió migración vertical en varias escalas temporales a medida que un frente de baja concentración fue rápidamente transportado a tasas de 100 a 500 m/año por delante de una pluma principal de movimiento más lento, la cual avanzó a tasas de 0.2 a 0.8 m/año. Las concentraciones de soluto en el borde frontal de la pluma mostraron un alto grado de variabilidad espacial en distancias verticales cortas hasta el día 1000. Al final de la prueba se hizo evidente la influencia de difusión intersticial a medida que se desarrollaron patrones de concentración de tipo irregular a distribución más uniforme. Los cálculos muestran que la masa dentro del frente de la pluma de

Received: 11 February 2006 / Accepted: 7 May 2007

W. G. Harrar · B. Nilsson · K. E. Klint
Geological Survey of Denmark and Greenland,
Øster Voldgade 10, DK-1350, Copenhagen K, Denmark

L. C. Murdoch
Department of Geological Sciences,
Clemson University,
340 Brackett Hall, Clemson, SC, USA

Present address:
W. G. Harrar (✉)
DONG Energy,
Agern Allé 24–26, 2970, Hørsholm, Denmark
e-mail: wilha@dongenergy.dk
Tel.: +1-45-45170873
Fax: +1-45-45171281

 DOI 10.1007/s10040-007-0198-5

baja concentración corresponde a menos del 1% de la masa total de soluto. La simulación de curvas de avance usando un modelo simple de transporte advección-dispersión en una dimensión en medio poroso indica que el transporte vertical está controlado principalmente por advección. Además, los resultados indican que el transporte vertical de solutos en zonas reductoras y oxidadas del conglomerado glacial puede simularse adecuadamente usando un medio poroso equivalente.

Keywords Glacial till · Fractured confining unit · Tracer test · Mass flux · Travel times

Introduction

Glacial tills were once thought to provide a low-permeability blanket that protected aquifers from contaminants over large areas of northern Europe and North America. However, it is now recognized that ubiquitous fractures can greatly reduce the protective capacity of tills because they increase the hydraulic conductivity by up to several orders of magnitude and provide pathways through an otherwise tight barrier (Hendry 1982; Keller et al. 1986; Fredericia 1990). The discovery of contaminants in aquifers provided the first indication that the overlying tills were leaking (Jørgensen and Fredericia 1992; Fenlon and Moore 1998). Numerical simulations show that vertical transport of near-surface contaminants along a few fully penetrating fractures can severely impact the water quality of underlying aquifers (Harrison et al. 1992). These suspicions were confirmed by field and laboratory tests demonstrating that colloids and some solutes could be transported rapidly along fractures (McKay et al. 1993a; Hinsby et al. 1996; Jørgensen et al. 1998).

A common feature of surficial glacial tills is a major decrease in fracture density across the boundary between oxidized and underlying reduced zones (Hendry 1982; Ruland et al. 1991; McKay and Fredericia 1995; Klint and Gravesen 1999). Typically, this results in a significant decrease in the bulk hydraulic conductivity and degree of fracture connectivity at depth within the reduced zone. These results also indicate that the vulnerability of underlying aquifers to contamination from near surface sources is largely controlled by the flow and transport characteristics of the reduced zone. However, the behavior of flow and transport within the reduced zone of glacial tills has received little attention.

The few published investigations of controlled field-scale tracer tests in glacial tills have largely focused upon transport within the shallow oxidized zone, and most of these tests were performed under forced-gradient conditions. A series of trench-to-trench tracer tests conducted by D'Astous et al. (1989) and McKay et al. (1993a) documented the horizontal transport of colloids at rates of 2–>5 m/day, while solutes were transported at rates of 0.01–0.07 m/day. The retardation of solutes relative to the colloids is attributed to matrix diffusion. At the same site, a chloride plume originating from a landfill migrated horizontally within the shallow oxidized zone at rates of 0.01–0.027 m/day (McKay et al. 1998). Sidle et al. (1998) conducted a vertical tracer experiment in which the breakthrough of a conservative tracer introduced slightly below the ground surface was observed at 4 m depth within 11 h after initiation of the test. In a similar test, McKay et al. (1999) infiltrated a conservative tracer and a bacteriophage slightly below ground surface and monitored vertical transport at various depths within the oxidized till. The bacteriophage was transported vertically at rates up to 1.5 m/day, whereas the conservative tracer was transported at rates of 0.007–0.05 m/day. Common to the controlled tracer tests, is the observed increase in the spatial variability of initial tracer arrival and concentrations with increasing travel distance and long tailing of solute breakthrough curves indicative of transport through complex fracture networks and matrix diffusion.

The presence of hydraulically active fractures at depth in reduced tills has largely been deduced from groundwater level monitoring, hydraulic tests and geochemical indicators of recent recharge (Hendry 1982; Ruland et al. 1991; Jørgensen and Fredericia 1992). Observations in a large excavation documented the occurrence of free-phase DNAPL in fractures to 9 m depth within a reduced till, providing direct evidence of transport along fractures (Jakobsen and Klint 1999). In a forced-gradient test, Nilsson et al. (2001) documented that a conservative tracer was transported through a 13-m thick glacial till to an underlying sand aquifer within 21 days after the tracer was applied at the ground surface. Solutes where also observed to be rapidly transported to a sand lens within the reduced zone of a glacial till during a short-term tracer test conducted under ponding conditions by Jørgensen et al. (2004). While these investigations have documented that solutes can be transported at environmentally significant rates along fractures within reduced glacial tills, plume development within the reduced zone has not been studied. This is largely because the published accounts of tracer tests in the reduced zone of glacial tills were conducted over relatively short time periods (weeks), and the monitoring of tracer breakthrough relied upon the sampling of effluent either in an underlying aquifer or sandy zones within the till rather than within the reduced zone itself.

This paper presents the results of a detailed investigation carried out in a fractured till at the Danish Institute of Agricultural Sciences research station (Flakkebjerg) located about 100 km south-west of Copenhagen on the island of Zealand. Activities performed at the site include fracture mapping in large excavations, hydraulic testing, and the monitoring of groundwater levels and a conservative solute tracer over 4.5 years. An innovative monitoring system installed at the site provided a detailed vertical profile of hydraulic heads and solute concentrations within both the oxidized and reduced zones. The objective of this paper is to integrate these observations into a conceptual model that describes the effects of the fracture system, hydraulic gradients and the bulk hydraulic properties on vertical transport within the oxidized and reduced zones of a surficial

 DOI 10.1007/s10040-007-0198-5

glacial till. Solute concentration data are also modeled using a simple theoretical analysis in order to identify the dominant processes governing vertical transport.

Methods

Piezometers

Nests of Shelby-hole type piezometers were installed following the procedure outlined by D'Astous et al. (1989). A total of 41 wells (Fig. 1b) were completed in the till at depths from 2 to 10 meters below ground surface (mbgs) and consist of 63-mm-ID PVC standpipe with piezometer tip lengths (screened interval) ranging from 0.25 to 0.5 m. Boreholes were drilled with a hollow stem auger (100 mm ID) and the lower portion of the borehole was advanced with a Shelby tube (70 mm diameter) in order to minimize smearing around the piezometer tip. The tip was installed in the hole created by the Shelby tube, and overlain by a thin layer of sand (10 cm). The borehole was then sealed with bentonite to the ground surface. These wells were used for hydraulic tests, groundwater level measurement and plume monitoring. Twelve cores measuring 42×140 mm were also obtained during drilling for laboratory determination of matrix permeability and porosity. An additional 17 standpipe piezometers (40 mm ID) were installed by hand augering to depths ranging from 2 to 2.8 m; completed with a 0.5 m piezometer tip and sealed with bentonite to the ground surface. These were used for plume and groundwater level monitoring. A standpipe piezometer (63 mm PVC) well was installed in the top of the underlying aquifer by drilling with a 125-mm hollow stem auger, installation of a 1-m piezometer tip and sealing of the borehole with bentonite. This well was used for hydraulic tests, groundwater level measurement and plume monitoring.

Sidewall samplers

An additional borehole was instrumented with 15 piezometers (sidewall samplers) embedded in the till through the wall of a 200-mm borehole. The sidewall samplers consisted of a porous polyethylene filter measuring 4 cm in diameter and 7 cm in length, and each sampler was accessed by two access tubes (3 and 6 mm OD) that allow for the measurement of groundwater levels and obtaining water samples. The sidewall samplers were spaced vertically every 25 cm from 2.25 to 4.25 mbgs in the upper and lower oxidized zones and at depths of 5.5, 6, 7, 7.25, 7.4 and 8 mbgs in the reduced zone. Murdoch et al. (2000) present further details about the sidewall samplers.

Hydraulic characteristics

The hydraulic conductivity of the till was determined by performing a series of falling and rising head slug tests and analyzing the results using the method of Hvorslev

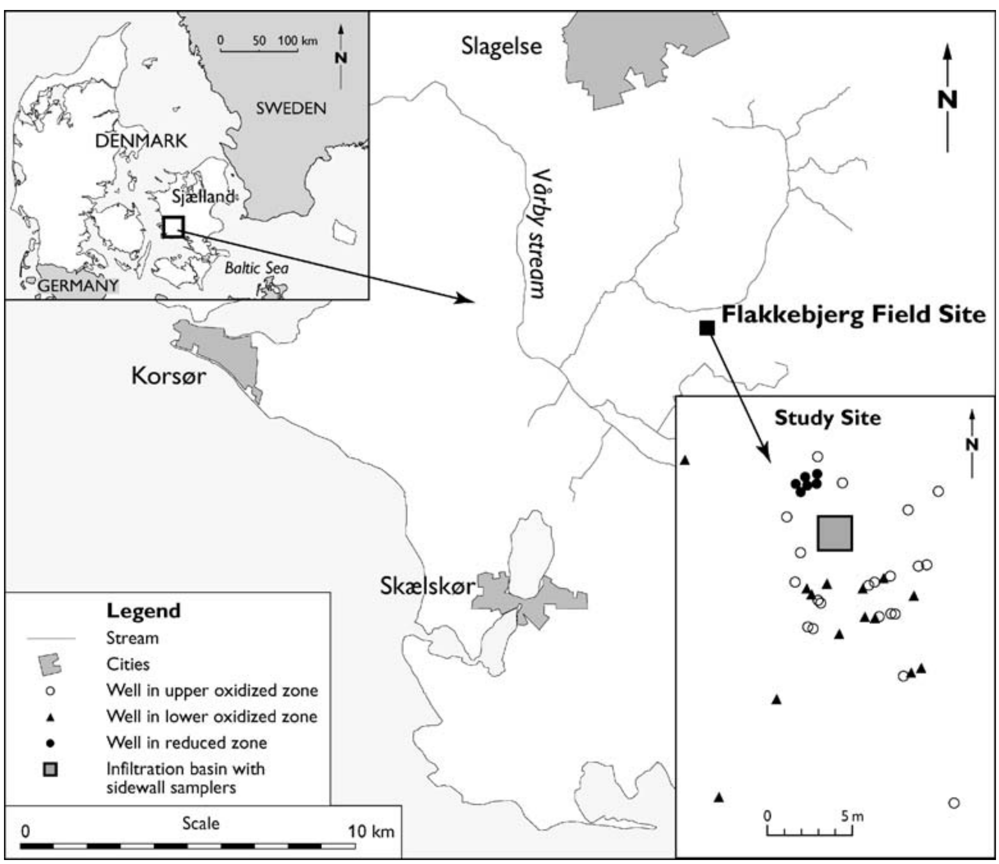

Fig. 1 Location of the study site, and distribution of wells at the facility

DOI 10.1007/s10040-007-0198-5

(1951). The hydraulic conductivity and total porosity of the matrix was determined in the lab on core samples collected during drilling. The hydraulic conductivity was determined as a specific liquid permeability in a special Hassler core holder. The total porosity was determined using a double-chambered Helium porosimeter with digital readout. Both methods are described in detail in Rosenbom et al. (1998). A pumping test conducted by Jones (1999) was designed to determine the hydraulic diffusivity of the till.

Tracer test

In preparation for the tracer test, an infiltration basin measuring 2×2 m was excavated to 2-m depth around the borehole containing the sidewall samplers. A column of glacial till measuring 0.5×0.5 m was left intact in the center of excavation surrounding the borehole containing the sidewall samplers. A 10-cm thick layer of gravel was placed in the bottom of the excavation on top of which drainpipe (100 mm ID) was installed. A PVC standpipe (15-cm ID) was connected to the drainpipe to allow for the introduction of freshwater and tracer to the infiltration basin. The excavation was backfilled with gravel and a shed was constructed over the basin to inhibit the infiltration of precipitation. This setup allows for the introduction of tracer directly into the upper oxidized zone, bypassing the bioturbated unsaturated zone, in order to investigate the vertical and horizontal transport of solutes that make it to the water table from the root zone.

An aqueous KBr solution (C_0=10,000 mg Br^-/L) was introduced into the infiltration basin in December 1997. The high bromide concentration was chosen to increase the likelihood of detecting early arrivals at depth in the till and underlying aquifer. The density of the tracer was approximately 4% greater than that of the ground water and it is possible that this density contrast caused the downward velocity of the tracer to be greater than that of the ambient flow. However, the choice of initial tracer concentration was a compromise between the requirement of being able to detect low concentrations of bromide at deeper levels in the reduced zone and effects of density driven flow along the plume front. A slug of tracer (3,000 L) was infiltrated over a 22-day period with an infiltration rate of 34 mm/day, followed by the infiltration of 8,000 L of freshwater over an additional 158 days (~12.7 mm/day). Groundwater levels inside the basin were maintained at about 20 cm over ambient groundwater levels during infiltration. This head difference is well within the range of observed, naturally occurring fluctuations in groundwater levels. Thus, the experiment was conducted under enhanced flow conditions for 180 days, and under naturally varying conditions for the remainder of the test. Originally, the tracer test was designed to characterize the vertical transport of a solute slug in the till over a 6-month period, and the freshwater was infiltrated in order to maintain steady-state flow conditions during this period. The decision to monitor the long-term development of the plume was made after the 6-month period had expired.

Monitoring

Groundwater levels were measured over a 3-year period in standpipe piezometers in the aquitard and the underlying aquifer using electric drop lines and over shorter time periods using pressure transducers and data loggers. Groundwater levels in the sidewall samplers were measured periodically using an electric drop line consisting of a 3-mm (OD) coaxial cable. Rainfall and barometric pressure were also monitored onsite.

Plume development was monitored over a 1,743-day period. Vertical migration of the bromide tracer in the oxidized and reduced zones was monitored by sampling the sidewall samplers using suction to lift water through the 3 mm diameter tubing. This results in small stagnant volumes (20–40 ml) that were purged prior to retaining a sample for analysis. The horizontal migration of the bromide plume in the oxidized till was monitored by periodically sampling the standpipe piezometers installed around the infiltration basin. Bromide concentrations were measured using an ion-selective probe (Phoenix Electrode Co., USA) with a detection limit of approximately 3 mg Br^-/L and a Dionex 500 ion chromatograph with a detection limit of 0.02 mg Br^-/L. Good agreement was found between concentrations measured using these two techniques. Analytical precision of bromide detection was ±2% with the ion selective probe and ±1% with the ion chromatograph.

Field site and geology

The Flakkebjerg site is located at the Danish Institute of Agricultural Sciences research station located about 100 km southwest of Copenhagen on the island of Zealand (Fig. 1). The geology of the area consists of a thick sequence of Pleistocene glacial and interglacial sediments underlain by Palaeocene limestone and clay. The field site is located on an undulating till plain of Late Weischelian age that covers an area of approximately 250 km^2.

The average annual precipitation is approximately 620 mm of which about 360 mm is lost by evapotranspiration. Interflow and discharge through drains is estimated to be approximately 210 mm/year, and recharge to the aquifer underlying the till is estimated to be 40–74 mm/year (Troldborg 2004), which is representative of the range of estimated recharge to regional aquifers in central and eastern parts of Denmark. Precipitation and evapotranspiration vary throughout the year with the greatest recharge occurring from late autumn through the winter.

Stratigraphy

This study focuses on a till sequence that extends 10–11 mbgs and overlies a regional sand aquifer deposited in the late Weischelian (18,000–14,000 years *BP*). The aquifer is a 10-m-thick layer of fine to medium-grained glacio-fluvial Tsands deposited on an outwash plain. The overlying till consists of basal lacustrine sediments overlain successively by a lower till, meltwater deposits and an upper till, according to detailed mapping in two 5.5-m-deep

DOI 10.1007/s10040-007-0198-5

excavations and cores from 32 borings at the site (Klint and Gravesen 1999).

The basal lacustrine sediments consist of 1–2 m of interbedded, dark olive gray clay, silt and fine-grained sand. The "lower till" is a 6–8-m-thick unit composed of massive, $CaCO_3$-enriched sediment composed of clay (15%), silt (40%), sand (38–42%) and gravel (3–7%). The lower till is a loam, according to the United States Department Agriculture classification based on grain size distribution, and internal sediment structures suggests it was deposited beneath a glacier as a lodgement till. The boundary between the oxidized and reduced zones occurs in the lower till at a depth of roughly 4.5 m and is marked by a color change from dark olive grey to olive brown.

The lower till is overlain by a meter-thick unit of olive brown, stratified sandy clay that contains deformed, discontinuous beds of sand and clay. This is termed the "meltwater unit" and is interpreted to have been deposited in fluvial and lacustrine settings.

The top of the stratigraphic column consists of an "upper till", 1–1.5 m thick, containing clay (10–15%), silt (20–25%), sand (57–63%) and gravel (3–7%). The upper till is an olive brown sandy loam with gray mottling. The $CaCO_3$ content of lower part of this unit is roughly 20%, whereas the upper part is completely reworked by bioturbation and devoid of $CaCO_3$. The soil horizon is 0.5-m-thick and consists of organic rich, bioturbated sandy, silty clay with minor gravel and cobbles.

Fractures

The formation of fractures at the field site can be related to the depositional history of the tills during two glacier advances/retreats and subsequent climatic changes during the Quaternary period. The fractures are separated into four systems: (1) large subvertical fractures related to the oldest glacier advance or interstadial climatic influence; (2) subhorizontal fractures related to subglacial drag/shear during a glacial advance from northeast and in an initial stage of a younger glacier advance from southeast; (3) normal faults related to subglacial loading during a late stage of the youngest glacier advance; (4) minor desiccation and freeze-thaw fractures related to post-glacial climatic influence (Klint and Gravesen 1999). Tills of glacial origin cover a large part of northern Europe and North America and many of these deposits have fracture characteristics similar to those observed at the Flakkebjerg site (Krüger and Kjær 1999 and McKay and Fredericia 1995).

The orientation, density and extent of the fractures vary significantly with depth (Fig. 2). No single fracture system penetrates the entire thickness, but the different systems crosscut to create an interconnected network throughout the till. Fractures in system 1 are subvertical and cut downward from the base of the oxidized zone presumably to the underlying aquifer. The average fracture spacing decreases with depth from 0.14 m at 3 mbgs to approximately 1 m at 5.5 mbgs. The strike of these fractures is roughly E–W. Reddish brown halos envelop these fractures, suggesting that oxidizing water has flowed through them.

System 2 fractures are gently dipping features that occur from 1.5 m to greater than 5.5 mbgs and cut across the system 1 fractures. The dips of these fractures range up to 25°, and their spacing is at most 0.5 m within the upper 5.5 m. Fractures in the upper part of this interval, between 1.5 and 3.5 mbgs, are nearly horizontal and, within the meltwater sediments from 2 to 3 mbgs, spacings are particularly close (~0.05 m).

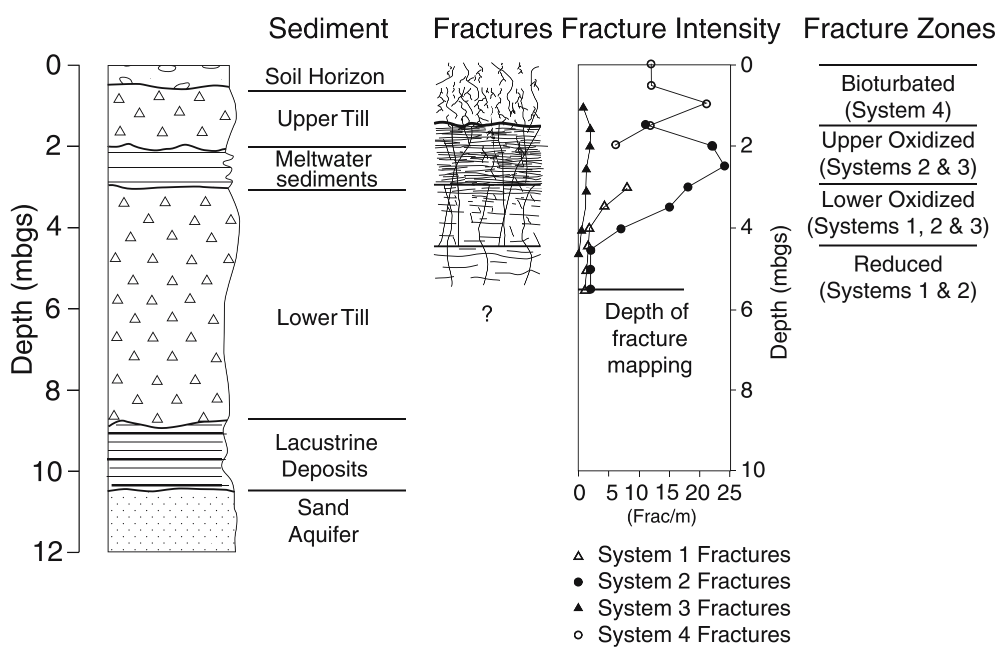

Fig. 2 Stratigraphic column and distribution of fractures

 DOI 10.1007/s10040-007-0198-5

System 3 consists of high-angle fractures and normal faults in the oxidized zone. These fractures strike NE–SW and are spaced roughly 0.5 m apart. They terminate at the base of the oxidized zone near 4 mbgs and their upper limit is roughly 1.5 mbgs. These are dominant fractures having wider oxidation halos and a higher density of roots on fracture surfaces than the other fracture systems.

System 4 fractures are subvertical and extend from the ground surface to approximately 2 mbgs. Strikes of these fractures are highly variable and many appear to be polygonal. Fracture spacing is less than 0.1 m. Worm and root holes are also common at shallow depths with system 4 fractures.

The fracture network consists of three sets of vertical fractures, systems 1, 3 and 4, and one shallowly dipping set, system 2, that cuts across them. Detailed mapping in a deep excavation showed that the extents of the vertical fractures systems are limited, but the upper extent of system 1 overlaps with the lower extent of system 3, and the upper extent of system 3 overlaps with the lower extent of system 4. The strikes of the vertical fracture systems differ, so some of the vertical fractures of one system will locally intersect those of the adjacent system. However, the extent of these intersections is limited, and probably represents only a contribution to the connectivity of the network. The gently dipping fractures of system 2 provide the major connectivity between the vertical fracture systems at the site.

Hydrostratigraphic units

Six hydrostratigraphic units can be defined based on geologic features and hydrologic behavior. The upper three units are in the oxidized zone and include the bioturbated, upper oxidized, lower oxidized zones. The underlying reduced zone includes an upper, middle and lower hydrostratigraphic unit.

The "bioturbated unit" extends from the ground surface to 1.5 mbgs and has a high density of wormholes, root holes and vertical desiccation fractures (system 4). It consists of the soil horizon and top of the upper till, and $CaC0_3$ is absent in the matrix.

The "upper oxidized unit" extends from about 1.5–3 mbgs, and consists of the upper till and meltwater deposits zone. It has the highest density of fractures, including the upper part of system 3 and the lower part of system 4, which are crosscut by closely-spaced, sub-horizontal fractures in system 2. The hydraulic conductivity of the entire oxidized zone ranges from 4×10^{-8} to 4×10^{-7} m/s, with an average value of 2×10^{-7} m/s.

The "lower oxidized unit" extends from the base of the upper oxidized zone (3 mbgs) to the top of the reduced zone (4–4.5 mbgs) and consists of the uppermost part of the lower till. It contains subvertical fractures from systems 1 and 3, cut by shallowly dipping fractures in system 2. The lower oxidized zone is distinguished from the upper zone by a decrease in the density of gently dipping fractures. Nevertheless, the hydraulic conductivity of the lower oxidized zones is similar to that of the upper zone, at least according to the results of slug tests (Fig. 3).

The reduced zone extends from the bottom of the lower oxidized zone to the top of the underlying aquifer at roughly 10 mbgs. The upper contact of the reduced zone is marked by a gradational color change from brown to gray between 4.0 and 4.5 mbgs. Hydraulic conductivity decreases across the contact from an average value of 2×10^{-7} m/s in the oxidized zone to 3×10^{-8} m/s in the upper reduced zone. The hydraulic conductivity of an interval from 7 and 8 mbgs is less than that in the overlying and underlying material, and this low *K* zone will be referred to as the "middle reduced unit". This low *K* unit was detected by slug tests, and it also is apparent in hydraulic head and concentration measurements made during the tracer test. The composition of the middle and upper reduced units are similar in core samples, and it appears that the difference in hydraulic conductivity results from changes in the connectivity of horizontal and vertical fracture sets. In general, the reduced zone includes system 1 and system 2 fractures, but the middle reduced zone was below the bottom

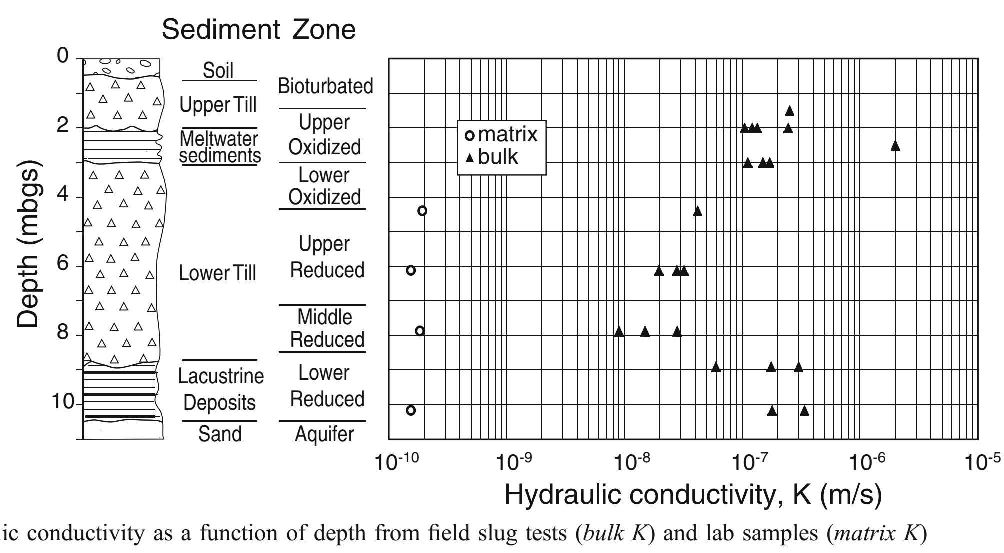

Fig. 3 Hydraulic conductivity as a function of depth from field slug tests (*bulk K*) and lab samples (*matrix K*)

of the excavation so the details of the connectivity of fractures in this zone could not be observed. The "lower reduced zone" includes lacustrine sediments below 9 mbgs, and has K values of about 6×10^{-8} to 3×10^{-7} m/s.

Hydraulic conductivity of the matrix was determined in the laboratory and values are in the range of 1×10^{-10} to 2×10^{-10} m/s. These values are two to three orders of magnitude less than bulk K values obtained from slug tests. This suggests that fractures occur throughout the till. Matrix porosity was also determined from laboratory samples, and it decreases from 0.20 to 0.44 in the oxidized zone to 0.17 to 0.25 in the reduced zone.

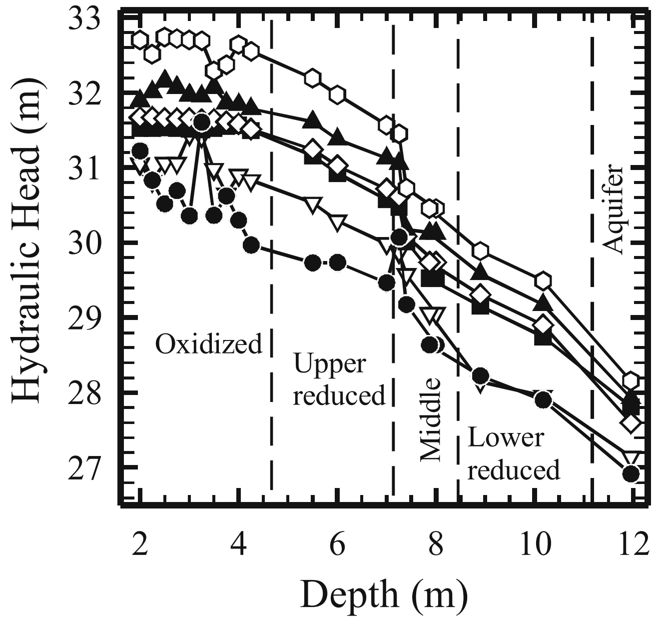

Fig. 5 Hydraulic head (m above sea level) profiles in the till over the range of values of head in the aquifer. *Filled circles*: 9/18/2000; *open triangles*: 30/7/1998; *filled squares*: 25/6/1998; *open diamonds*: 18/11/1999; *filled triangles*: 25/2/2000; *open circles*: 11/3/1999

Results

The behavior of the tracer was evaluated by first characterizing the flux of water and then evaluating transport. Vertical profiles of hydraulic heads were used to calculate hydraulic gradients, and vertical fluxes were calculated using Darcy's Law. The rate of advance of the tracer plume was determined by establishing the position of the leading edge of the plume, and the position of the center of mass as functions of time.

The time series tracer data were simulated using a simple one-dimensional advection-dispersion model in order to shed light upon the processes controlling vertical transport in the till. These results were integrated into a conceptual model describing vertical transport in the till.

Hydraulic heads and water flux

Groundwater levels fluctuated seasonally during the study period, attaining their highest elevations within the bioturbated zone during the winter, and their lowest levels within the lower oxidized zone in the autumn (Fig. 4). The magnitude of annual groundwater level fluctuations decreased with depth from over 2.5 m in the oxidized zones to 1.5 m in the reduced zone and underlying aquifer.

Head fluctuations also occurred on a shorter timescale, with piezometric levels increasing abruptly by as much as 0.5 m in response to rainfall during the winter and spring. These head perturbations traveled through the till to the underlying aquifer in less than 1.5 days, according to detailed tests described by Jones (1999). The short-term response to rainfall seems to change with season, however, because the record from conventional piezometers (Fig. 4) shows few fluctuations in the summer and autumn when piezometric levels were falling. The details of this effect are complicated, however, because a different response occurs in the sidewall piezometers, where head perturbations apparently resulting from rainfall events are observed throughout the year.

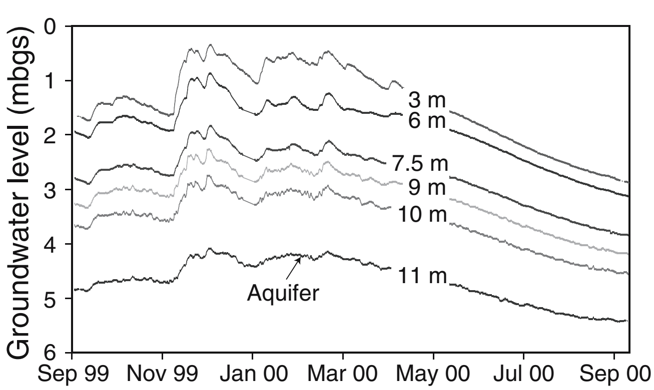

Fig. 4 Groundwater levels in D-series piezometers as a function of time

Head profiles

Vertical profiles of hydraulic head maintained roughly the same shape while differing in magnitude through most of the annual cycle of head variation in the aquifer, according to 27 measurements from the sidewall piezometers over 1,000 days (Fig. 5). In general, the oxidized zone was characterized by uniform heads with mild gradients at some times, and spatial variability with steep local gradients at other times. The high spatial variability appears to be the spatial manifestation of the short-term temporal fluctuations accompanying rainfall events shown in the hydrograph when water levels are high (Fig. 4).

Hydraulic heads drop with depth and the gradient in the reduced zone is steeper than in the overlying oxidized zone (Fig. 5). The head gradient is particularly steep across the middle reduced unit. Head perturbations within the reduced zone, inferred to be related to rainfall events, appear to be dampened compared to those in the oxidized zone, although significant perturbations were observed in the reduced zone. For example, the hydraulic head is

DOI 10.1007/s10040-007-0198-5

Table 1 Vertical hydraulic head gradients, conductivities and calculated fluxes

Hydrostratigraphic unit	Monitoring well series	Vertical gradient mean	Standard deviation/coeff. of variation	K min $\times10^{-7}$ m/s	K max $\times10^{-7}$ m/s	q_v m/year	95% Con. m/year
Oxidized	Sidewall	-0.09	0.13/1.5	1.00	2.50	0.27	0.16
Upper reduced	Sidewall	-0.37	0.12/0.3	0.20	0.35	0.24	0.03
Middle reduced	Sidewall	-0.99	0.45/0.4	0.09	0.30	0.28	0.05
Lower reduced	D	-0.46	0.22/0.5	0.60	3.00	0.86	0.16
Entire till	D	-0.38	0.03/0.08	0.25	0.59	0.30	0.01

Abbreviations: *Coeff.* coefficient; *Con. confidence intervals*

anomalously high at the top of the middle reduced zone in the profile marked by filled circles (Fig. 5).

The hydraulic head profile when the head in the aquifer is particularly low appears to differ from the profiles when the aquifer head is higher. The low-head profile shown as filled circles in Fig. 5 is characterized by a steepening of the head gradient in the oxidized zone and a flattening in the middle reduced zone. This produces a head gradient that is nearly uniform through the till when water levels in the aquifer are low.

Head gradients

Head gradients were determined by regression using the head measurements within a particular hydrostratigraphic unit. Average hydraulic head gradients ranged from a low of 0.09 within the oxidized unit to a high of roughly 1.0 in the middle reduced unit (Table 1). The average gradients within the upper and lower reduced units were 0.36 and 0.45, respectively. For comparison, the gradient was roughly uniform across the entire till and equal to 0.45 when the head in the aquifer was low (circles in Fig. 5). Variability in the head gradients is σ=0.12–0.23, except within the intermediate reduced zone where the variability is greater with σ=0.45 (Figs. 5 and 6). Much of this variability appears to occur when head distributions containing non-linear perturbations are fit by linear regression.

The hydrograph data (Fig. 4) and the head profiles (Fig. 5) suggest that the till during high heads behaves differently when the heads are falling or low. Groundwater levels throughout the till fluctuate in response to short-term rainfall events when the hydraulic heads are high, whereas they decline uniformly during falling or low-head conditions. However, head gradients determined by regression fail to show seasonal periodicity (Fig. 6). This suggests that the seasonal effects that produced variations in the hydrograph and head profiles have a limited effect on the head gradients. It is expected that the head gradients do vary seasonally, but the seasonal change in gradient is less than the variability resulting from short-term perturbations accompanying rainfall events.

Volumetric flux

Vertical fluxes were determined as the product of hydraulic head gradient and hydraulic conductivity. It seems reasonable to use the lower estimate of the hydraulic conductivity for each unit because this value will limit the flux through the unit. This gives a remarkably consistent range of 0.24–0.28 m/year for the flux through the upper three units. Confidence intervals (95%) based on variability of the head gradient measurements are less than 0.05 m/year in the upper and middle reduced unit. The uncertainty in the oxidized zone is

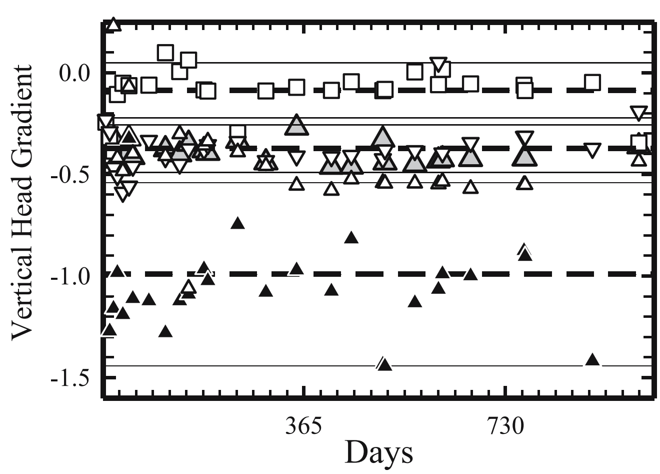

Fig. 6 Vertical hydraulic head gradient as function of time from the slope of the best-fit line through sidewall piezometer data from the oxidized zone (*squares*), upper oxidized zone (*downward triangles*), middle reduced zone (*black triangles*), and lower reduced zone (*open upward triangles*). The gradient from the upper and lower D piezometers in the till is represented by the *large gray triangles*. *Dashed lines* are the mean values for each zone, and *solid lines* are one standard deviation

 DOI 10.1007/s10040-007-0198-5

greater, 0.16 m/year, as a result of the larger variability in head gradient in this zone.

The flux through the lower reduced unit is predicted to have been several times greater than the overlying units, but this is due to a larger hydraulic conductivity estimated for that unit. It seems likely that the hydraulic conductivity of the lower reduced unit was over estimated because of the proximity of the underlying aquifer. The bulk *K* for each unit ranged over roughly a factor of three, so the fluxes could be as much as three times larger than the values given above and in Table 1.

Vertical flux across the entire till was calculated by another approach that used only two measurements. The head gradient was determined using one piezometer at the top of the till and another at the top of the aquifer, and the hydraulic conductivity of the till was determined as the harmonic mean of the values obtained at different depths (Fig. 3). By comparison, each of the other gradients was calculated using best-fit lines through between 3 and 10 head measurements at different depths. The average head gradient across the entire till is −0.38. The standard deviation obtained using this approach is remarkably small, only 0.03. Flux determined using the simple method is 0.3 m/year, which was calculated using the minimum bulk hydraulic conductivity (K_{min}=2.5×10^{-8} m/s) for the entire till sequence. Interestingly, the simple method for determining vertical flux gives values that are essentially the same as the more detailed measurements in individual zones.

The piezometer data indicate that the average flux of water through the reduced zone of the till is 0.28 m/year, using the low end of the ranges of hydraulic conductivity measurements. The 95% confidence interval for the flux estimates in the upper and middle reduced zones, and for the overall till is 0.05 m/year or less (Table 1). Seasonal variations in flux probably do occur, but they are small and obscured by the fluctuations caused by individual rainfall events. This suggests that the seasonal variation in flux is less than 0.05 m/year.

Vertical transport

Vertical transport of bromide was determined using the relatively closely spaced sidewall samplers along with some conventional samplers. The initial concentration of the bromide tracer was C_0=10,000 mg Br^-/L and this value will be used to scale the results to a relative concentration.

Concentration profiles

The concentration increased throughout the till within 1–2 days after the tracer was applied (Fig. 7). Background concentration increased from 5×10^{-5} to 10^{-4} to more than 0.01 throughout the upper oxidized zone (3 m) within 1 day. The tracer rapidly penetrated much deeper than this, with concentrations of 10^{-3} at the tops of both the upper reduced unit (4 m) and middle reduced unit (7.25 m) within 2 days. These three depths where tracer was

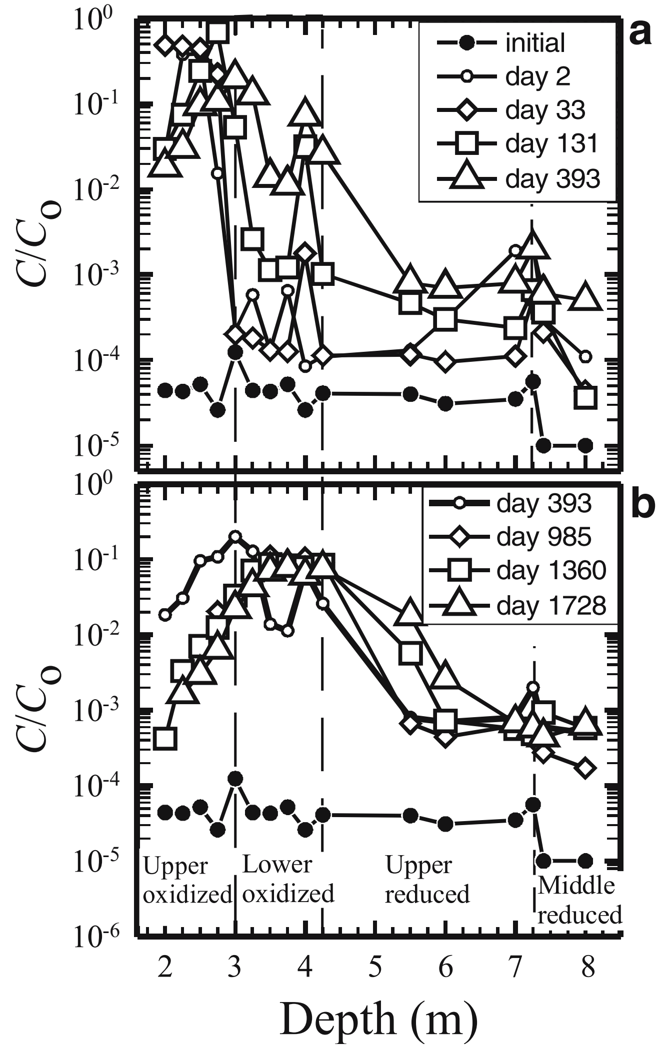

Fig. 7 Normalized concentration profiles during approximately the first **a** year since tracer release, and **b** 4.5 years since release

observed during the first few days would remain as active "reservoirs" of tracer throughout the test.

The primary reservoir of tracer moved downward into the lower oxidized zone during the first year of the test (Fig. 7a). During the first month of the test, tracer concentration decreased to background values ahead of the primary reservoir, but it increased with depth as a secondary reservoir of tracer accumulated at the top of the reduced zone. Concentrations decreased beneath the secondary reservoir, but increased again at a tertiary reservoir on the top of the middle reduced unit (Fig. 7a).

Tracer was replaced with freshwater on day 22 and concentrations in the trailing edge of the primary tracer reservoir began to diminish soon thereafter (Fig. 7a). Nevertheless, the front of the primary reservoir and the concentration and width of the secondary reservoir continued to increase. Concentrations at greater depth in the tertiary reservoir decreased to roughly background values soon after freshwater was applied, but they increased and fluctuated after that. Concentrations at the

DOI 10.1007/s10040-007-0198-5

top of the middle reduced unit continued to exceed those in the underlying and overlying samplers.

Total mass

The mass of tracer beneath the source area was determined by integrating the concentration profiles as a function of depth at different times. This gives the total mass of tracer per unit area in plan view. The total mass increased abruptly to 0.4 gm/m^2 and then decreased to 0.2 gm/m^2 during the first 270 days. Freshwater was injected into the tracer delivery pit until day 180, and the reduction in mass during the first 270 days probably is because the tracer was spread laterally in the oxidized zone by the fresh water. The total mass was variable in the range of 0.2 gm/m^2 during the next 2 years, but then it decreased from 0.21 to 0.15 gm/m^2 during the last 2 years of the test.

It is possible that the total mass in the plume decreased during the last 2 years because tracer was being transported through the till to below the sampler at 8 m. Alternatively, tracer could have been transported laterally, just as it was during the first 270 days.

The mass of tracer in the three reservoirs was determined separately and scaled to the total mass at each measurement time. These results show the mass in the oxidized zone decreases while that in the reduced zone increases, and the two masses are equal after approximately 4 years (Fig. 8b). Interestingly, the rates of change of normalized masses in the two reservoirs are fast for the first 730 days, the time when the total mass is decreasing. However, the rates of change of the normalized masses are roughly uniform after day 730, when the total mass in the system decreases.

The normalized mass in the lower reservoir, at the top of the middle reduced unit, remained extremely small throughout the experiment. The normalized mass increased during the test (even though the scale in Fig. 8 masks this change) and reached a maximum of 0.005.

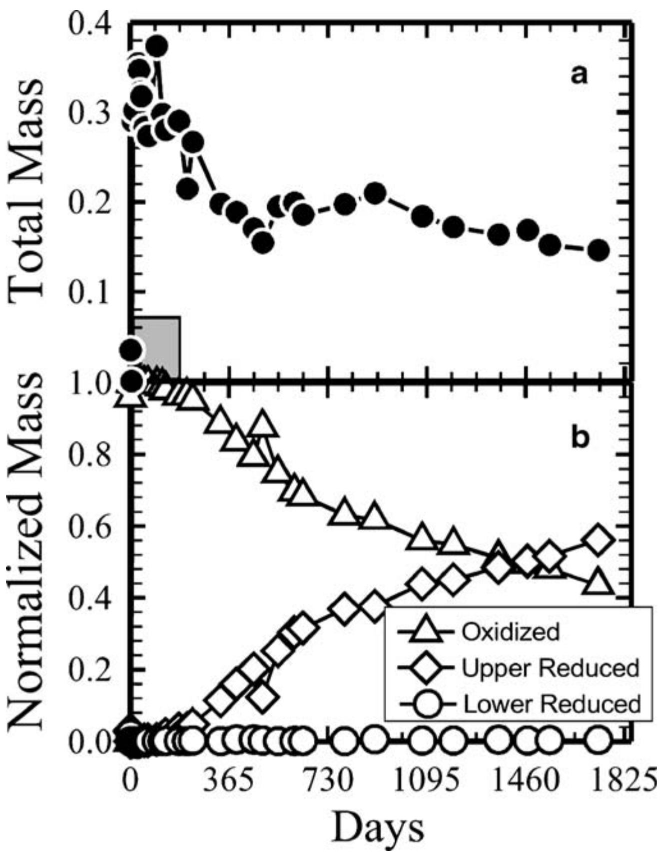

Fig. 8 **a** Total mass per unit area in the plume below the source (*filled circles*) as function of time. The *shaded rectangle* shows the duration of water injection; and **b** distribution of mass among the different reservoirs shown as mass in each reservoir normalized to the total mass in the plume at that particular time

Breakthrough

Breakthrough curves show the peculiar behavior of the multiple tracer reservoirs (Fig. 9). Concentrations in the oxidized unit increased and then fall (open circles in Fig. 9), with the arrivals becoming increasingly delayed and peaks increasingly diminished with depth. The concentrations in the reduced zone behaved similarly (filled circles in Fig. 9), except that the concentrations arrive at the top of the reduced zone early in the test and remained greater than concentrations in overlying samplers in the lower oxidized zone (e.g. large open circles from the sampler at 3.5 m). For clarity, only a few of the data sets are shown in Fig. 9.

This behavior seems to be repeated at the top of the middle reduced zone, where tracer arrived early in the test and concentrations remained roughly equal to 0.001 during the first year. The concentration fell to 10^{-4} during the second year, however, perhaps as a result of dilution by the freshwater. Concentration increased to 4×10^{-3} and then diminished to roughly 5×10^{-4} for the duration of the test. Within the middle reduced unit, at 8 mbgs, tracer remained at background concentrations during the first

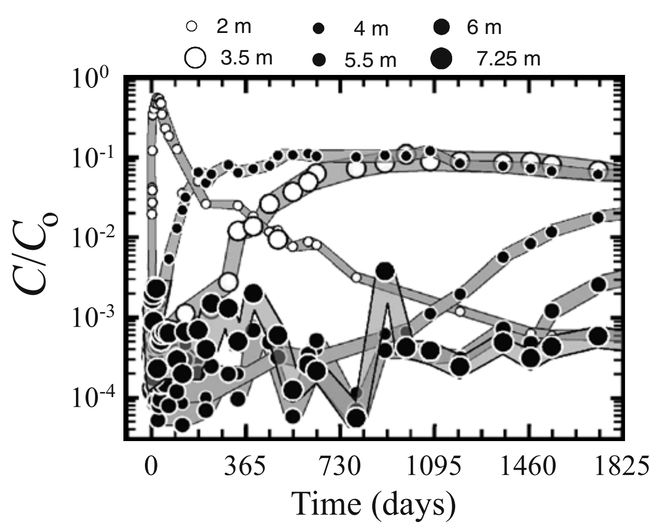

Fig. 9 Concentration as functions of time and depth at selected sidewall samplers. Water injection ended on day 180. The *shading* is the tie lines between the data points

DOI 10.1007/s10040-007-0198-5

year but it increased thereafter and all the samples from the middle confining unit (7.25, 7.4 and 8 mbgs) contained roughly the same concentration of tracer after day 1,000, although these data are not shown.

Rate of advance

The rate of advance of the tracer plume was determined by establishing the position of the leading edge of the plume, and the position of the center of mass as functions of time. The times when tracer concentrations of C=0.01 and C=0.001 first arrived at particular locations were determined from the breakthrough curves for each sampler. The results show the arrivals of C=0.001 at the three hydrostratigraphic contacts occurs within a few days after the start of the test (Fig. 10). These data give transport velocities of 1–5 m/day for low concentrations of tracer to reach all three of the reservoirs at contacts within the till.

The arrival time data can be misleading, however, because by no means did the tracer arrive everywhere within the till within a few days. In general, arrival times increased with depth below the top of each reservoir. For example, the tracer arrived at 2.75 m within 2 days, but it took another year for the C=0.01 front to penetrate to 3.5m. Moreover, concentrations reached 4m within a few days, but it would take roughly 4 years for the concentration front to reach 5.5 m. (Fig. 10). The concentrations below the top of the middle reduced zone increased, but they remained below C=0.001, so the curve can only be estimated in this region.

The arrival times can be fitted with straight lines with slopes that are approximately the same for the two concentration levels, but that differs between the two hydrostratigraphic units. The velocity of the tracer front can be determined as the inverse of the slopes of these lines. The velocity of the front of the primary tracer reservoir was approximately 0.9 m/year, whereas the secondary reservoir advanced at roughly 0.4 m/year. These velocities appear to be roughly constant. For comparison, the initial arrival of tracer moved at velocities of 500–1,000 m/year.

The movement of the tracer can also be evaluated by determining the center of mass as a function of time. This was done by integrating the concentration profiles to determine the first moment of the concentration at 33 times during the test. The center of mass was calculated for the total plume, as well as the plumes in the oxidized and the reduced zones. During approximately the first 400 days, the center of mass of the total plume advanced at approximately 0.75 m/year as the plume migrated vertically in the upper oxidized zone (Fig. 11). The rate of advance slowed and advanced at approximately 0.2 m/year after roughly day 500, once the plume reached the lower oxidized zone and advanced at a near constant rate thereafter (Fig. 11). The center of mass of the plume in the oxidized zone was essentially the same as the total plume during the early, relatively rapid advance. After day 500, the center of mass of the oxidized plume lagged behind the total center of mass which had migrated from the upper to the lower oxidized zones, yet the two centers of mass advanced at about the same rate. Interestingly, the rapid advance of the small amount of tracer that initially composed the reduced plume caused its center of mass to be quite low and then move upward. This upward movement essentially stopped and the location of the center mass in the reduced zone remained constant once

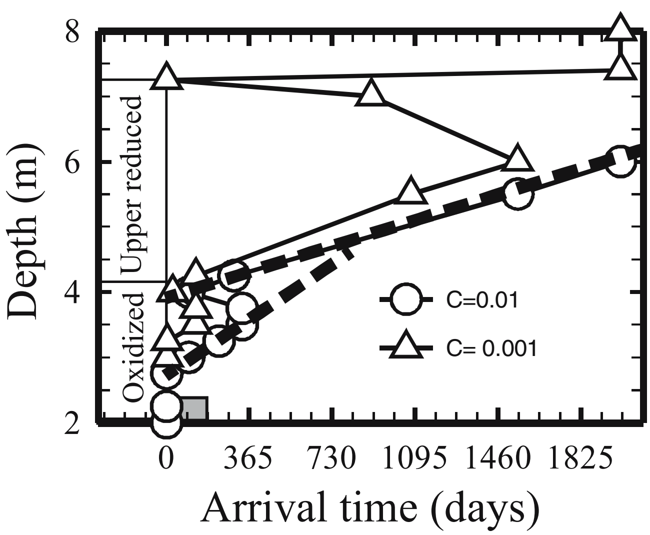

Fig. 10 Depth of C=0.01 and C=0.001 front as a function of arrival time. *Dashed lines* are best fits to C=0.01 data in the oxidized and reduced zones. The *shaded rectangle* shows the duration of water injection

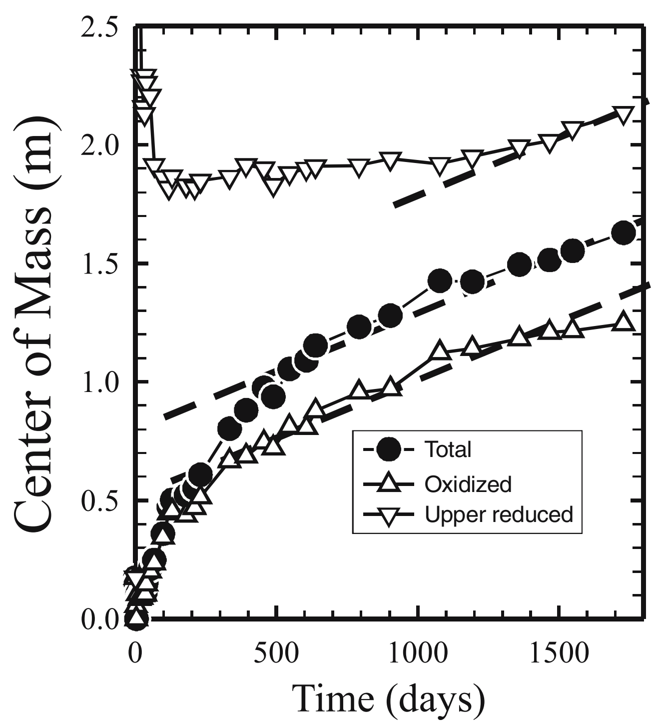

Fig. 11 Displacement of the center of mass (below 2.2m depth) of the total plume, and the plumes in the oxidized and reduced zones as functions of time. *Dashed reference line* is equivalent to slope 0.18 m/year

DOI 10.1007/s10040-007-0198-5

the total center of mass had migrated downward from the upper oxidized zone into the lower oxidized zone. Late in the test, however, after day 1,400, the center of mass of the reduced plume moved at the same rate as the other centers of mass, roughly 0.2 m/year. This coincides with the migration of the total center of mass to the bottom of the lower oxidized zone.

Bromide concentrations at a depth of 11 m at the top of the underlying aquifer remained at background levels (0.08 mg Br^-/L or C/C_o=0.000008) until day 297, when concentrations there increased by a factor of 2. This apparently was the first arrival of the tracer in the aquifer, and it is roughly two orders of magnitude later than the first arrival at 7 m depth in the till. This large difference in arrival times could result from a significant reduction in velocity at the bottom of the aquitard, however, a more likely explanation is that it is due to the relative performance of the samplers. Water samples were obtained from the top of the aquifer using a conventional piezometer with a 1-m-long screen embedded in the sand 2 m north and slightly hydraulically upgradient of the array of sidewall samplers. Tracer recovered from the conventional piezometer in the aquifer is probably diluted much more than when it is recovered from the sidewall samplers. Tracer reaching the aquifer as a dilute and fast plume, and then flowing along a single stream tube, could be diluted by an order of magnitude or more when it reached the conventional monitoring well in the aquifer below the infiltration basin. An alternative explanation could be that either the solute reached the aquifer through a fracture as depicted in Fig. 12d and therefore was not sampled directly by the well, or there might have been a lateral hydraulic gradient that could have sent the Br plume away from the well once it reached the aquifer. Concentrations in the aquifer continued to increase slightly during the remainder of the test, and the highest values were a factor of 5 greater than background levels.

Periodic fluctuations in concentration were superimposed on the systematic changes resulting from bulk downward transport. Bromide concentrations throughout the till varied in response to groundwater level fluctuations at the seasonal and rainfall event scales. Maximum annual concentrations in the lower oxidized zone occurred during the late summer months of all 3 years of the test. Groundwater levels were also lowest at these times. Concentrations in the upper oxidized zone decreased abruptly as the water levels increased each year in early winter. In contrast, the highest concentrations in the reduced zone occurred during winter and spring when groundwater levels were high. Concentrations in both the lower oxidized and reduced zones varied erratically with temporary drops in concentration observed in samples collected immediately after periods of heavy rainfall.

Theoretical analysis

The bromide breakthrough curves were simulated using a simple one-dimensional advection-dispersion model of transport in porous media. The objective of the modeling exercise was to identify the dominant processes governing the bulk vertical transport of solutes in the till. The tracer release was simulated by assuming that the concentration is known beneath the bromide release pit, and that this concentration is given by

$$C_o = D_p; \qquad t < t_f \tag{1}$$

$$C_o = C_p e^{-\lambda(t-tf)}; \qquad t < t_f \tag{2}$$

where t_f is the time when clean water was flushed into the bromide pit. A solution to the boundary conditions given above was obtained by superimposing analytical solutions given on pages 11 and 19 of van Genuchten and Alves (1982).

The data were analyzed using a Levenberg-Marquardt algorithm to estimate the parameters that minimize residuals between predicted values and the concentration time series for each sampler. All of the solute breakthrough curves were fitted simultaneously, yielding a single set of parameter estimates that describe the bulk vertical transport in the till. The parameter estimation process produced functions that fit the data fairly well, with an average r^2 value of 0.7. The results show that the

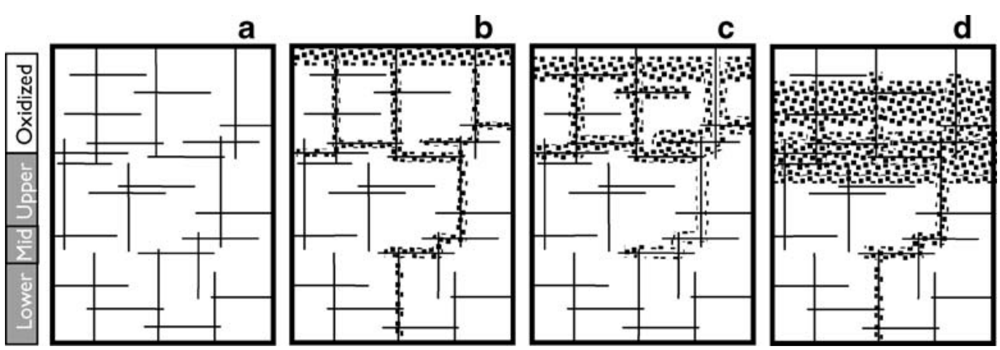

Fig. 12 Conceptual model of the Flakkebjerg tracer test. **a** Initial fracture network relative to hydrostratigraphic units; **b** initial application of tracer; **c** early fracture dominated transport; **d** late matrix diffusion dominated transport

 DOI 10.1007/s10040-007-0198-5

retardation is relatively low, indicating that the retardation of bromide in the till is minor. The average velocity is 0.002 m/day. The vertical flux was estimated to be about 7×10^{-4} m/day. This gives a value of about 0.3 for the effective porosity when using the average velocity. The estimated effective porosity is within the range of matrix porosity values measured in the laboratory.

The average dispersion coefficient is 8.9×10^{-4} m^2/day. The diffusion coefficient of Br in water is 1.7×10^{-4} m^2/day, and using a tortuosity of 0.3 gives an effective diffusion constant of 5×10^{-5} m^2/day.

The ratio of the longitudinal dispersion to the molecular diffusion in this system is 18. The Peclet number was determined using the depth of the sampler below the bottom of the bromide source (2 m) as the characteristic length. This gives an average Peclet number of 3.5 and indicates that advection and dispersion are more important than diffusion in the transport of bromide through the till. The average dispersivity is 2 m.

The results of the theoretical analysis indicate that vertical transport of the tracer is dominated by advection. Furthermore, the results indicate that vertical transport of solutes in the till appears to be adequately simulated using an equivalent porous media (EPM).

Discussion

Much has been learned as a result of research during the past 20 years about how compounds are transported through tills, but novel monitoring methods were used during the Flakkebjerg test that further refine this understanding. The conceptual model that results from this test recognizes that fast transport paths exist along fractures through the till, but significant solute reservoirs occur at interfaces along these paths and affect the overall mass flux.

The flow of water and transport of solutes appear to be controlled by the details of the fracture network in the till. The Flakkebjerg till includes at least three sets of vertical fractures contained within different depth ranges and with different strikes. The bottom of one fracture set overlaps slightly with the top of the underlying set, so a few of the vertical fractures may locally intersect those in an overlying or underlying set. However, most of the connectivity between vertical sets of fractures appears to occur through horizontal fractures that cut across them. System 3 fractures overlap with system 1 fractures at a depth of roughly 4 m, which is location of the secondary tracer reservoir at the contact between the oxidized and reduced zones. Fracture systems 4 and 3 overlap at a depth of approximately 2 m, which is where the tracer was released. A fourth set of vertical fractures probably occurs below approximately 7 m and is responsible for the behavior of the middle reduced zone.

An idealized representation of the fracture network consists of different sets of vertical fractures of restricted height linked together by horizontal fractures (Fig. 12a). Pathways that traverse the till follow a vertical fracture downward to its lower termination, and then turn along a horizontal fracture and progress laterally until intersecting another vertical fracture from an underlying set. Some pathways probably extended through the entire till thickness at Flakkebjerg, but only after encountering at least two intervals, at 4m and 7m, requiring horizontal transport from one set of vertical fractures to another. These are intervals where tracer concentrations were observed to increase as mass accumulated ahead of the main plume. As a result, the regions where horizontal fractures connect vertical fractures act as reservoirs of tracer.

It appears that within a day or two after release, the tracer moves along a pathway and starts to accumulate in reservoirs associated with horizontal connecting fractures at 4 and 7m (Fig. 12b). It seems likely that some tracer probably also reached the aquifer at this time. Tracer was first detected in the aquifer nearly 300 days later, this is most likely because the fast path through the till only allowed minute amounts of tracer mass to penetrate and this mass was diluted to less than detectable concentrations until day 297.

The main reservoir of tracer progressed downward in the upper oxidized zone at a velocity of about 0.8 m/year during the first year. However, transport along vertical fractures continued to actively move tracer ahead of the front of the main reservoir, and increase the mass stored in the reservoir at 4 m (Fig. 12c). The tracer was chased with freshwater, and rainfall provided additional freshwater, which caused tracer concentrations to decrease at some locations. The rate of advance of the main reservoir slowed to approximately 0.2 m/year after roughly 500 days and advanced at a near constant rate thereafter. Concentrations in the lower oxidized and reduced zones displayed a high degree of spatial variability over short vertical distances through day 1,000.

Late in the test, the effects of matrix diffusion become readily apparent as concentrations patterns throughout the till develop from being irregular to smoother, more uniform distributions (Fig. 12d). The bulk of solute mass within the oxidized and upper reduced zones moves at the same rate of about 0.2 m/year and this velocity is similar to the downward volumetric water flux. The fast transport paths remain active, but account for a minute fraction of the moving mass.

Simulation of the solute breakthough curves with a simple one-dimensional advection-dispersion model shows that transport of the main solute plume is dominated by advection. The results indicate that transport rates of the main solute plume are controlled by the bulk hydraulic conductivity and an effective porosity, which is slightly less than the lowest values measured for the matrix. These results also indicate that transport of the bulk of the solute mass in the oxidized and reduced zones can be simulated using an equivalent porous media (EPM) modeling approach and average hydraulic conductivities. Previous studies have shown that EPM methods are applicable for simulating solute transport within the oxidized zone of tills where the fracture density is high, but are less effective in simulating solute transport at

 DOI 10.1007/s10040-007-0198-5

depth in tills where fractures are widely spaced such as in the reduced zone (Sidle et al. 1998, Jørgensen et al. 1998, McKay et al. 1993a, b). The results of this study appear to differ from those of previous investigations by indicating that the EPM method may be applicable for simulating solute transport in the reduced zone even where the fracture spacings are relatively large (0.5–1 m). However, it is important to note that in this study, the vertical transport of a solute was monitored over a period of years, whereas as the tracer tests performed by Sidle et al. (1998), Jørgensen et al. (1998) and McKay et al. (1993a, b) were conducted over much shorter time periods (weeks to months).

The results of this study suggest that the effects of discrete fractures are important when explaining the results of short-term tracer tests such as those cited above, but transport over time scales of years can be described using the EPM approach. This suggestion is supported by Helmke et al. (2005), who performed forced gradient tracer tests on intact columns of till in the laboratory and analyzed the results using numerical models. Their simulations with EPM and discrete fracture models are very similar, and both can explain the tracer results under longer time scales and realistic hydraulic gradients. However, they also show that EPM assumptions can be inappropriate for short temporal scales (days to months) and at a length scales where fracture spacing is greater than the experimental test volume (or smaller than REV) such as in the reduced zone of tills.

The conclusion about the applicability of EPM models to transport through tills is apparently at odds with Jørgensen et al. (2004), who conducted 3-month-long forced-gradient laboratory experiments with flow rates ranging between 11 and 49 mm/day and samples that were 0.5 m long. Jørgensen et al. (2004) concluded that discrete fracture, rather than EPM, numerical models were required to explain the results of their lab experiments. However, the scales of the flow rates, sample lengths, and durations of the Jørgensen et al. (2004) experiments differ from the in-situ scales of the Flakkeberg test by 1–2 orders of magnitude. Those scale differences suggest that the results of Jørgensen et al. (2004) are inapplicable to the field study at Flakkebjerg.

The solute tracer in the till at the Flakkebjerg site was observed to migrate vertically at two different rates as a low-concentration front advanced ahead of the more slowly moving main plume. These observations are consistent with numerical studies of flow and transport in low-permeability fractured media which show that fractures control the position of the leading edge of solute plumes and bulk hydraulic properties control the bulk movement of solute mass (Sudicky and McLaren 1992; Harrison et al. 1992; Therrien and Sudiky 1996). These modeling studies also show that the mass flux in fractures is very small compared to that of the matrix, indicating that the slow moving main plume in fractured glacial tills represents the greatest threat to water quality in underlying aquifers. The results of this study indicate that the EPM modeling approach is appropriate for simulating the long-term migration of solutes through glacial tills to underlying aquifers.

The rapid early arrivals of tracer at depth in the reduced zone may have been influenced by density effects associated with initial concentrations of the solute tracer. The initial concentrations were necessary to produce a distinct signal when the tracer arrived at the samplers. Analyses to evaluate the effects of tracer density are planned for future work.

The Flakkebjerg tracer test benefited from advances in monitoring and characterization techniques to produce data that refines the conceptual model for solute transport through till. Sidewall samplers (Murdoch et al. 2000) were emplaced at vertical spacings that were closer than could be achieved using vertical wells. Moreover, each sampler was embedded in the formation instead of contained within a wellbore, and the purge volume of the sidewall samplers was a small fraction of short-screened sampling wells. As a result, the sidewall samplers provided higher spatial resolution, more representative concentration measurements, and disrupted the formation less than conventional samplers.

Summary and conclusions

The results of the tracer test show that solutes migrated vertically at several different time scales during the course of the experiment. Concentrations increased throughout the upper oxidized zone within the first day of the test, while a low concentration front was rapidly transported to depth within the lower oxidized and reduced zones at rates of 1–5 m/day. The depths where the tracer was observed during the first few days remained as active reservoirs of tracer throughout the test. During the first year of the test, the center of mass of the main plume in the upper oxidized zone migrated vertically at a rate of about 0.8 m/year, while the center of mass in the reduced zone moved slightly upward and then moved very slowly downward. Concentrations in the lower reservoirs fluctuated showing the continued rapid transport of solutes to depth in the till. Concentrations in the underlying aquifer increased above background levels after about 300 days and continued to increase throughout the test, confirming connectivity of the fracture network across the thickness of the till. The rate of advance of the main plume decreased to about 0.2 m/year as it descended into the lower oxidized zone after about 500 days and remained constant thereafter. Concentrations in the lower oxidized and reduced zones displayed a high degree of spatial variability over short vertical distances through day 1,000. Late in the test, the effects of matrix diffusion become readily apparent as concentrations patterns throughout the till developed from being irregular to smoother, more uniform distributions. The bulk of solute mass within the oxidized and upper reduced zones moves at the same rate of about 0.2 m/year and this velocity is similar to the downward volumetric water flux. The fast-transport paths remain active, but account for a minute fraction of the moving mass.

This investigation provides some of the first detailed vertical profiles of groundwater levels and solute transport within the oxidized and reduced zones over a time period of several years. The study benefited from detailed mapping at the site, which revealed the various geometries and connectivities of the fracture systems. The fracture network is idealized as consisting of different sets of vertical fractures of restricted height linked together by horizontal fractures which create vertical hydraulic connectivity across the entire thickness of the till. The conceptual model recognizes that fast-transport paths exist along fractures through the till, but significant solute reservoirs occur at interfaces along these paths and affect the overall mass flux.

Simulation of the vertical transport of the solute tracer using a simple one-dimensional advection-dispersion model shows that advection is the dominant process governing the bulk transport of the solute mass and that transport rates are controlled by the average hydraulic conductivity of the till. This is consistent with the calculations showing that the mass in the plume front, which arrived in the lower reduced zone at early times and persisted for the duration of the test, accounts for less than 1% of the total mass. These results support the hypothesis presented by Helmke et al. (2005) that solute transport in glacial tills over a time scale of years can be reliably simulated using an EPM modeling approach.

Tills provide important barriers to the contamination of underlying aquifers, and predicting the effectiveness of these barriers is important for managing groundwater resources in glaciated areas. The EPM modeling approach used here is based on bulk hydraulic properties that can be obtained from relatively simple field studies. The implications are that it may be feasible to combine the EPM approach with simple field data to develop reliable predictors of the rates at which tills in different areas will allow contaminants to reach underlying aquifers.

Acknowledgements The project was financed by the Danish Government under the National Strategic Environmental Research Programme (SMP96). Additional funding was given by the Geological Survey of Denmark and Greenland (GEUS). The authors gratefully acknowledge J. C. Refsgaard for his constructive suggestions for improving the manuscript and the field, laboratory and office assistance of P. Jensen, E. Clausen, J. Morthorst, K. Rasmussen and R. Hodges. M. Helmke, D. Daly and K-P. Seiler are also thanked for their critical and insightful reviews of the manuscript. The opinions expressed in this paper are solely those of the authors and do not necessarily reflect those of DONG Energy.

References

D'Astous AY, Ruland WW, Bruce, JGR, Cherry JA, Gillham RW (1989) Fracture effects in the shallow groundwater zone in weathered Sarnia-area clay. Can Geotech J 26:43–56

Fenlon, JM, Moore, RC (1998) Transport of agrichemicals to groundwater and surface water in a small central Indiana watershed. J Environ Qual 27:884–894

Fredericia J (1990) Saturated hydraulic conductivity of clayey tills and the role of fractures. Nord Hydrol 25:119–132

Harrison B, Sudicky EA, Cherry JA (1992) Numerical analysis of solute migration through fractured clayey deposits into underlying aquifers. Water Resour Res 28(2):515–526

Helmke MF, Simpkins WW, Horton R (2005) Simulating conservative tracers in fractured till under realistic timescales. Ground Water 43(6):877–889

Hendry MJ (1982) Hydraulic conductivity of a glacial till in Alberta. Ground Water 20(2):162–169

Hinsby K, McKay LD, Jørgensen PR, Lenczewski M, Gerba CP (1996) Fracture aperture measurements and migration of solutes, and immiscible creosote in a column of clay-rich till. Ground Water 34(6):1065–1075

Hvorslev MJ (1951) Time lag and soil permeability in ground-water observations. US Army Corps Eng Bull 36:50

Jakobsen PR, Klint KES (1999) Fracture distribution and occurrence of DNAPL in a clayey lodgement till. Nord Hydrol 30(4/5):285–300

Jones EH (1999) Hydraulic characterization of a fractured clayey till, western Zealand, Denmark. MSc Thesis, Department of Geology, University College of London, UK

Jørgensen PR, Fredericia J (1992) Migration of nutrients, pesticides and heavy metals in fractured clayey till. Géotechnique 42:67–77

Jørgensen PR, McKay LD, Spliid NH (1998) Evaluation of chloride and pesticide transport in a fractured clayey till using large undisturbed columns and numerical modeling. Water Resour Res 34(4):539–553

Jørgensen PR, Helstrup T, Urup J, Seifert D (2004) Modeling of non-reactive solute transport in fractured clayey till during variable flow rate and time. J Contam Hydrol 68 (3–4):193–216

Keller CK, van der Kamp G, Cherry JA (1986) Fracture permeability and groundwater flow in clayey till near Saskatoon, Saskatchewan. Can Geotech J 23:229–240

Klint KE, Gravesen P (1999) Fractures and biopores in Weichselian clayey till aquitards at Flakkebjerg, Denmark. Nord Hydrol 30 (4/5):267–284

Krüger J, Kjær KH (1999) A data chart for field description and genetic interpretation of glacial diamict and associated sediments: with examples from Greenland, Iceland and Denmark. Boreas 28:386–402

McKay LD, Fredericia J (1995) Distribution, origin, and hydraulic influence of fractures in a clay-rich glacial deposit. Can Geotech J 32:957–975

McKay LD, Gillham RW, Cherry JA (1993a) Field experiments in a fractured clay till. 2. Solute and colloid transport. Water Resour Res 29(12):3879–3890

McKay LD, Cherry JA, Gillham, RW (1993b) Field experiments in a fractured clay till. 1. Hydraulic conductivity and fracture aperture. Water Resour Res 29(4):1149–1162

McKay LD, Balfour DJ, Cherry JA (1998) Lateral chloride migration from a landfill in a fractured clay-rich glacial deposit. Ground Water 36(6):988–999

McKay LD, Fredericia J, Lenczewski M, Morthorst J, Klint, KES (1999) Spatial variability of contaminant transport in a fractured till, Avedøre, Denmark. Nord Hydrol 30(4/5):333–360

Murdoch LC, Slack W, Harrar W, Siegrist RL (2000) Embedded sidewall samplers and sensors to monitor the subsurface. Ground Water 38(5):657–664

Nilsson B, Sidle RC, Klint KES, Bøggild CE, Broholm K (2001) Mass transport and scale-dependent hydraulic tests in a heterogeneous glacial till-sandy aquifer system. J Hydrol 243:162–179

Rosenbom A, Aamand, J, Friis K, Lindgreen H, Springer N (1998) Laboratory setups and experimental results: progress report. In: Pore-to-core scale-up studies of the transport properties of organic pollutants with natural attenuation. Geological Survey of Denmark and Greenland Report No. 104, GEUS, Copenhagen

Ruland WW, Cherry JA, Feenstra S (1991) The depth of fractures and active ground-water flow in a clayey till plain in southwestern Ontario. Ground Water 29(3):405–417

Sidle RC, Nilsson B, Hansen M, Fredericia J (1998) Spatially varying hydraulic and solute transport characteristics of a fracture till determined by field tracer test, Funen, Denmark. Water Resour Res 34(10):2515–2527

Sudicky EA, McLaren RG (1992) The Laplace transform Galerkin technique for large-scale simulation of mass transport in discretely fractured porous formations. Water Resour Res 28(2):499–514

Therrien R, Sudicky EA (1996) Three-dimensional analysis of variably-saturated flow and transport in discretely-fractured porous media: model development and illustrative examples. J Contam Hydrol 23(1–2):1–44

Troldborg L (2004) The influence of conceptual geological models on the simulation of flow and transport in Quaternary aquifer systems (in English). PhD Thesis, Geological Survey of Denmark and Greenland Report No. 107, GEUS, Copenhagen

van Genuchten MT, Alves WJ (1982) Analytical solutions of the one-dimensional convective-dispersive solute transport equation. US Department of Agriculture, Tech Bull 1661:151

 DOI 10.1007/s10040-007-0198-5